Journal of Cerebral Blood Flow & Metabolism (2014) 34, 1522–1530

www.jcbfm.com

ORIGINAL ARTICLE

3-Nitropropionic acid-induced ischemia tolerance in the rat brain is mediated by reduced metabolic activity and cerebral blood flow

Oliver Bracko[1], Valentina Di Pietro[2], Giacomo Lazzarino[3], Angela M Amorini[3], Barbara Tavazzi[3], Judith Artmann[1], Eric C Wong[4,5], Richard B Buxton[4], Michael Weller[1], Andreas R Luft[1] and Susanne Wegener[1]

Tissue tolerance to ischemia can be achieved by noxious stimuli that are below a threshold to cause irreversible damage ('preconditioning'). Understanding the mechanisms underlying preconditioning may lead to the identification of novel therapeutic targets for diseases such as stroke. We here used the oxidative chain inhibitor 3-nitropropionic acid (NPA) to induce ischemia tolerance in a rat middle cerebral artery occlusion (MCAO) stroke model. Cerebral blood flow (CBF) and structural integrity were characterized by longitudinal magnetic resonance imaging (MRI) in combination with behavioral, histologic, and biochemical assessment of NPA-preconditioned animals and controls. Using this approach we show that the ischemia-tolerant state is characterized by a lower energy charge potential and lower CBF, indicating a reduced baseline metabolic demand, and therefore a cellular mechanism of neural protection. Blood vessel density and structural integrity were not altered by NPA treatment. When subjected to MCAO, preconditioned animals had a characteristic MRI signature consisting of enhanced CBF maintenance within the ischemic territory and intraischemic reversal of the initial cytotoxic edema, resulting in reduced infarct volumes. Thus, our data show that tissue protection through preconditioning occurs early during ischemia and indicate that a reduced cellular metabolism is associated with tissue tolerance to ischemia.

Journal of Cerebral Blood Flow & Metabolism (2014) **34,** 1522–1530; doi:10.1038/jcbfm.2014.112; published online 18 June 2014

Keywords: acute stroke; animal models; ASL; brain imaging; MRI

INTRODUCTION

The ability of an organism to develop tolerance against stressful conditions can help to survive temporary restrictions in energy supply, low oxygenation, or other environmental challenges. Among other organs, the brain can acquire tolerance to experimental injury such as trauma or ischemia.[1] In human stroke, the immediate onset and time-dependent course of damage have driven the search for rapid neuroprotective measures. The interest in ischemia tolerance was fueled by clinical observations that a brief episode of ischemia such as a transient ischemic attack of the brain or preinfarction angina of the heart, might protect against subsequent stroke or heart attack, similar to experimental preconditioning.[2–4] To study mechanisms involved in ischemia tolerance, several experimental preconditioning strategies have been described *in vivo* and *in vitro,* such as hypoxia, brief episodes of ischemia, or oxygen-glucose deprivation.[5–8] Some of the mechanisms identified include attenuation of excitatory damage through reduced glutamate release and downregulation of NMDA receptors, changes in gene expression patterns favoring neuroprotection, as well as neurorestorative responses such as the induction of neural progenitor cells. Although vascular adaptations in response to preconditioning could help to facilitate substrate delivery during subsequent ischemia, the potential role of blood vessel remodeling in ischemia tolerance remains open.[5,9]

Our goal was to characterize mechanisms of preconditioning and to predict histologic and behavioral outcomes after stroke by defining a magnetic resonance imaging (MRI) signature of the ischemia-tolerant brain. We utilized a pharmacological preconditioning paradigm with the oxidative chain inhibitor 3-nitropropionic acid (NPA), which temporarily induces ischemia tolerance through inhibition of succinate dehydrogenase and a burst of reactive oxygen species.[10–14] Using longitudinal, quantitative arterial spin labeling (ASL)-cerebral blood flow (CBF) measurements, as well as structural MRI, we here show that ischemic damage and recovery evolve differently in ischemia-tolerant brains. CBF was significantly reduced in NPA-preconditioned rats at the time of ischemia tolerance, which was associated with decreased metabolic activity, as determined from the quantification of high energy phosphates in tissue obtained from NPA-treated and control rats. Thus, we here identify a cellular mechanism mediating preconditioning in the context of ischemic stroke.

MATERIALS AND METHODS

Preconditioning, Stroke Induction, and Experimental Groups

All experiments were performed in accordance with the National Institutes of Health animal protection guidelines and approved by the UCSD Institutional Animal Care and Use Committee. Adult male Wistar rats 280 to 310 mg body weight were used for all experiments.

[1]Department of Neurology, University Hospital Zurich, Zurich, Switzerland; [2]Division of Neurotrauma and Neurodegeneration, School of Clinical and Experimental Medicine, University of Birmingham, Birmingham, UK; [3]Institute of Biochemistry and Clinical Biochemistry, Catholic University of Rome, Rome, Italy; [4]Departments of Radiology, University of California San Diego, La Jolla, California, USA and [5]Departments of Psychiatry, University of California San Diego, La Jolla, California, USA. Correspondence: Dr S Wegener, Department of Neurology, University Hospital Zurich, Frauenklinikstrasse 26, Zurich 8091, Switzerland.
E-mail: Susanne.Wegener@usz.ch
We are grateful for support by the Swiss National Science Foundation: NCCR Neural Plasticity and Repair as well as the Marie Heim-Vögtlin Foundation, the Koetser Foundation, the European Union FP6 Marie Curie Outgoing International Fellowship, and the Deutsche Forschungsgemeinschaft.
Received 18 March 2014; revised 28 May 2014; accepted 29 May 2014; published online 18 June 2014

For preconditioning, NPA (20 mg/kg body weight) or the same volume of saline (controls) was injected once intraperitoneally. Three days after sham or NPA treatment, animals were subjected to 60 minutes of middle cerebral artery occlusion (MCAO). A modification of the Koizumi intraluminal filament method was applied.[15] During surgery and MRI, animals were anesthetized using facemask inhalation of 1.5 to 2.5% isoflurane in a 2:1 N_2O:O_2 atmosphere. Temperature was maintained at 37 °C by a feedback-controlled heating pad.

The first MRI (D0) was acquired during MCAO without discontinuation of anesthesia. For MRI, the animal was placed in a custom-built cradle. Body temperature and respiratory rate were continuously monitored during MRI sessions. After 60 minutes of MCAO, the occluding filament was removed and the animals allowed to recover. Animals were re-anesthetized for repetitive MRI at the following time points after MCAO: day 0 (D0), D1, D4, and D14 after MCAO. Vasodilatory capacity was assessed on D4 and D14 by comparing MRI-CBF measurements acquired under isoflurane anesthesia in room air ('air') with those acquired in a 5% CO_2 atmosphere ('CO_2'), after a 2-minute adjustment between switching gases as previously described.[16] Animals were sacrificed on D14 after the last MRI acquisition and brains subjected to further histologic analysis. The CBF maps obtained from the control group have been published elsewhere.[17] Functional assessments were obtained before each MRI session and in addition on D7 after MCAO. Of the initially included 21 animals, eight controls and five NPA animals remained in both groups; exclusions were because of massive stroke and intolerable weight loss/behavioral abnormalities/seizures: controls $n=3$, NPA $n=0$; because of surgical complications (subarachnoid hemorrhage upon advancement of the thread): controls $n=2$, NPA $n=1$; and because of behavioral abnormalities such as reduced spontaneous activity or failure to perform baseline functional assessment within predefined range (see below): controls $n=0$, NPA $n=2$. Another group of animals received either intraperitoneal NPA ($n=7$) or saline ($n=12$) treatment and MRI assessment was done 3 days later. After MRI, animals were sacrificed and brains extracted for further histologic analysis. A separate group of animals was treated with either NPA ($n=10$) or saline ($n=10$) and brains extracted for high-performance liquid chromatography (HPLC) analysis of brain energy rich phosphates 3 days later.

Magnetic Resonance Imaging Acquisition and Data Processing

Magnetic resonance imaging experiments were carried out on a 3 T GE Signa Excite whole-body system with a body transmit coil and a custom-built passively decoupled single-loop receive-only head coil. CBF imaging was achieved with multislice flow-sensitive alternating inversion recovery pulsed arterial spin labeling with the QUIPSS II modification.[18] In addition, diffusion-weighted imaging with generation of apparent diffusion coefficient maps and fractional anisotropy maps, as well as T1- and T2-weighted imaging were carried out. For details of the MRI sequences and analysis strategies please see also Wegener et al (2007 and 2013).[17,19]

Images from all animals at all time points were first co-registered and then averaged using codes written in Matlab (Mathworks, Natick, MA, USA) software. Vasoreactivity (VR) maps were generated by subtracting the CBF map acquired in air from the one acquired in 5% CO_2.

Voxels with significantly reduced apparent diffusion coefficient values were automatically selected as all voxels with a value of $<$mean + 2 s.d. of a contralateral hemisphere region of interest. Similarly, regions of interest for increased T2-values ($>$ mean + 2 s.d. contralateral on a T2 map) or hyperperfusion ($>$ mean + 2 s.d. contralateral on a CBF map) were selected. A voxel-wise independent sample *t*-test was used to compare CBF maps of NPA or with those of control animals with a threshold of $P<0.05$ using Matlab codes.

Behavioral Testing

Adhesive tape removal test: to assess sensorimotor function and neglect after MCAO, two strips of tape (18 × 12 mm) were applied in random order to the saphenous part of the forepaws. The time that the animals took to contact (sensory function/neglect) and remove (sensorimotor function) the tape on both sides (left and right) was recorded. Results from three trials at least 5 minutes apart were averaged at each session.[20,21]

The 18-point observational score for assessment of sensorimotor deficits after MCAO was also applied; results from this score for the control group have been previously published.[17,22] In this test, a maximum of three points is scored for each of the following observations: (1) spontaneous activity, (2) symmetry in limb movement, (3) forepaw outstretching, (4) climbing, (5) body proprioception, and (6) response to vibrissae touch, so that 18 points indicate no neurologic deficit.

Cerebral Tissue Processing and High-Performance Liquid Chromatography Analyses of Metabolites

An *in vivo* craniectomy was performed on all animals during anesthesia with the aid of an operating microscope. After carefully removing the rat's skull, the brain was freeze-clamped by aluminum tongues, pre-cooled in liquid nitrogen, and immediately immersed in liquid nitrogen, to accelerate freezing of the tissue and increase the recovery of metabolites.[23] After the wet weight determination, the brain was deproteinized according to the organic solvent deproteinizing procedure, described in detail elsewhere, which ensures no loss of labile compounds and guarantees an efficient deproteinization of the tissue for metabolite analysis.[24] Deproteinized samples were then filtered through a 0.45-μm HV Millipore filter (Millipore, Billerica, MA, USA) and loaded (20 μL) onto a Hypersil C-18, 250 × 4.6 mm, 5-μm particle size column, provided with its own guard column (Thermo Fisher Scientific, Milan, Italy). The column was connected to an HPLC apparatus consisting of a SpectraSystem P4000 pump system (Thermo Fisher Scientific) and a highly-sensitive UV6000LP diode array detector (Thermo Fisher Scientific) equipped with a 5-cm light path flow cell and set up between 200- and 300-nm wavelengths. Data acquisition and analysis were performed using a personal computer and the ChromQuest software package provided by the HPLC manufacturer. N-Acetylaspartate and metabolites related to tissue energy state and mitochondrial function (adenosine triphosphate (ATP), adenosine diphosphate (ADP), adenosine monophosphate (AMP), nicotinamide adenine dinucleotide) were separated, in a single chromatographic run, according to a gradient modification of existing ion-pairing HPLC method.[24,25] Assignment and calculation of the compounds of interest in chromatographic runs of tissue extracts were carried out at either 206 (N-Acetylaspartate) or 260-nm wavelength by comparing retention times, absorption spectra, and areas of peaks with those of peaks of chromatographic runs of freshly prepared ultrapure standard mixtures with known concentrations. The energy charge potential (ECP) in brain extracts was calculated according to the equation: ECP = ATP + 1/2ADP/ATP + ADP + AMP.

Immunofluorescence and Histochemistry

After perfusion fixation, brains were removed, immersed in ice-cold 4% formalin and transferred to 30% sucrose solution for at least 3 days. Coronal 40-μm-thick sections were cut on a freezing microtome (Leica, Nussloch, Germany). Every twelfth slice from each brain was stained for KCC2 and RECA-1 fluorescence intensity measurement. All sections were stained and imaged in parallel. Primary antibodies used were mouse α-RECA-1 1:400 (AbD Serotec, Oxford, UK), rabbit α-KCC2 1:500 (Millipore), α-rabbit CC3 1:400 (Bioconcept, Allschwil, Switzerland), α-rabbit GFAP 1:1000 (Sigma-Aldrich, Buchs, Switzerland), α-mouse MAP2 1:500 (Abcam, Cambridge, UK), α-mouse COX-IV 1:250 (Abcam). Secondary antibodies were goat α-mouse-Cy3 1:300 and goat α-rabbit-Alexa488 1:300 (Jackson ImmunoResearch, Suffolk, UK). Nuclei were counterstained with 4,6-diamidino-2-phenylindole (Sigma-Aldrich). Images were processed in Adobe Photoshop (CS5 for Mac) or ImageJ (NIH).

For DAB immunohistochemistry, endogenous peroxidase was quenched using 0.6% hydrogen peroxidase for 30 minutes at RT, after the regular staining protocol using mouse α-NeuN 1:200 (Millipore), α-ED1 1:1000 (AbD Serotec) as a primary antibody and mouse α-Biotin (1:250; Jackson ImmunoResearch) as a secondary antibody. DAB staining was done using VECTASTAIN Elite ABC Kit (Vector Laboratories, Burlingame, CA, USA) and DAB Peroxidase Substrate Kit, 3,3-diaminobenzidine (Vector Laboratories). Sections were mounted using DPX Mountant (Sigma-Aldrich).

Image Analyses

For fluorescence intensity quantification, images were taken using a × 20 objective with an inverted Leica Wide field microscope (Leica DMI 6000, Leica). ROIs (710 × 530 μm) were chosen from cortical and subcortical regions bilaterally, using the same settings for all conditions. The measurements from contralateral and ipsilateral ROIs were combined per section and animal. RECA-1 and KCC2 fluorescence intensity was measured and calculated using the ImageJ (NIH) software package as mean signal intensity/mm^2 ± s.d.

For the quantification of NeuN− DAB staining after stroke, areas showing loss of NeuN expression were derived by subtracting the manually outlined areas of intact NeuN+ staining on the ipsilateral side from the area of the contralateral hemisphere, thereby correcting for edema. The sum of all areas with loss of NeuN staining was multiplied by the distance between slices, deriving lesion volume in mm^3.

COX and KCC2 signal intensity were measured with a frame size of 1024 × 1024 pixels on a scanning confocal microscope (FluoView FV1000, Olympus, Tokyo, Japan) at a constant Z-step of 0.5 μm using a × 20 objective for COX and × 40 oil objective for KCC2. Quantification was done using ImageJ (NIH). All images were taken with the same laser power and gain settings. Pictures were taken contralateral and ipsilateral from a cortical, striatal, and dentate gyrus (DG) region, per section and animal. All pictures were analyzed in Imaris 7.6.3 (Bitplane, Belfast, UK) using the Imaris MeasurementPro package (Bitplane). The MAP2 signal was three-dimensionally reconstructed while using the same threshold settings for all images per region. The volume was calculated and the KCC2 intensity was extracted from the MAP2 three-dimensional reconstruction.

Statistical analysis

All statistical analyses were carried out in SPSS v12.0 for Windows, except for the voxel-wise *t*-test of CBF data (Figure 4A), which was performed in Matlab.

All values are given as mean ± s.d. For group comparisons, the two-sided independent sample *t*-test was used. In not normally distributed data, the nonparametric Mann–Whitney *U* test was used for group comparisons. Repeated measures general linear model analyses were conducted to assess significant differences between functional performances over time in control or NPA animals. A *P*-value < 0.05 was considered significant.

RESULTS

3-Nitropropionic Acid Preconditioning Results in Tissue Protection and Improved Functional Outcome after Middle Cerebral Artery Occlusion through Maintained Intraischemic Cerebral Blood Flow and Apparent Diffusion Coefficient Recovery

Experimental ischemia was induced by MCAO in adult male Wistar rats preconditioned with NPA or pretreated with saline. Fifteen minutes after occlusion of the MCA, ischemic lesions were readily detected on diffusion-weighted imaging, affecting cortical and subcortical areas within the occluded left MCA-territory in both groups (Figure 1A). Notably, in a second diffusion-weighted imaging acquisition 30 minutes later with the occluding device still in place, lesions had remained stable in controls, but had diminished in NPA-treated rats, where only one animal showed a significant reduction in the apparent diffusion coefficient after 45 minutes of ischemia (Figures 1A and 1B). Quantitative CBF imaging using arterial spin labeling showed a drop in CBF on the ischemic side during MCAO in both groups and a recovery of CBF after retraction of the occluding filament from D0 until D14 (Figure 2A). The perfusion restriction was, however, less severe in NPA animals (Figure 2B). Between D1 and D14, all animals of the control group showed a postischemic hyperperfusion, which was significantly attenuated and only detected on D1 in the NPA group (Figures 2A and 2C). This pattern of less extensive postischemic hyperperfusion with an earlier peak after reperfusion is an indicator of less severe ischemic damage.[17] Indeed, infarct size as determined from T2-weighted MRI on D14 was dramatically smaller in preconditioned animals (Figure 2D). Diffusion tensor imaging revealed that callosal and descending corticospinal fiber tracts were initially damaged, reflected by a hyperacute increase and subacute decrease in fractional anisotropy, but, in contrast to controls, regained structural integrity in the NPA group (Figure 2E).

The VR remained intact in NPA-preconditioned animals on D4 and D14 after MCAO. In contrast, the normal vasodilatory response to a 5% CO_2 stimulus was lost on the ischemic side in controls on D4 (Figures 2F and 2G). In most control animals, VR subsequently recovered or even showed an overshooting CBF increase on D14.

Magnetic resonance imaging findings correlated with improved functional performance. In a composite neurologic score, combining measures of sensory and motor function typically affected after MCAO, deficits were still detectable on D14 in controls, showing a significantly better performance of the NPA group at all observation time points (Figure 3A).

Deficits in sensorimotor function and neglect after MCAO were also assessed in the sticky tape test. The time to first contact and removal of the tape was measured. Before MCAO, animals were trained to remove the tape within 10 seconds. On D1 after left-sided MCAO, deficits to perceive and remove the tape on the right side were noted in all animals, causing an increase in the time to contact and remove the tape on the right forepaw (Figure 3B). Both groups showed a fast recovery towards D7. On average, NPA animals performed faster, which did, however, not reach significance in the repeated measures analysis of variance.

Tissue Protection by 3-Nitropropionic Acid Preconditioning

Next, we analyzed infarct size after MCAO in NPA-treated versus control rats. Loss of NeuN expression was significantly smaller in NPA than in control animals (13.3 ± 2.5 mm^3 versus 48.6 ± 11 mm^3; $P < 0.01$ Figures 4A–C). Strikingly, loss of NeuN expression occurred in most NPA animals without signs of tissue necrosis, whereas controls had undergone extensive cystic degeneration of brain tissue on the ischemic side (Figures 4A and 4C). In controls, infarct border zones were characterized by loss of NeuN staining, detection of cleaved caspase-3 (CC3) positive cells indicating apoptosis, an increase in GFAP signal because of gliosis, and an increase in RECA-1 signal corresponding to peri-infarct angiogenesis. Furthermore, macrophage infiltration around the infarct border zone was visible on ED1 immunohistochemistry (Figures 4A and 4D).

Neuronal death was observed in all NPA animals after MCAO in scattered cortical and subcortical regions, along with GFAP and

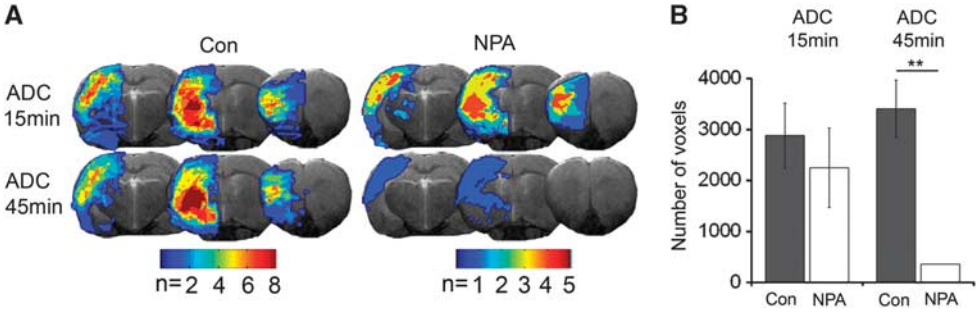

Figure 1. Intraischemic ADC recovery in NPA-preconditioned animals. (**A**) Masks of the ischemic lesion from individual animals of the control (Con) or NPA-treated group derived from ADC maps acquired 15 (upper panel) or 45 (lower panel) minutes after the onset of MCAO. Masks are overlaid onto anatomic (T2w) images. Regions of overlap between individual animals are color-coded. Although the area of ADC reduction is similar at 15 and 45 minutes ischemia duration in controls, there is a dramatic intraischemic recovery in the NPA group. (**B**) Number of voxels with a significantly reduced ADC (mean ± s.d.) at 15 and 45 minutes after the onset of ischemia (**$P < 0.01$). ADC, apparent diffusion coefficient; MCAO, middle cerebral artery occlusion; NPA, 3-nitropropionic acid.

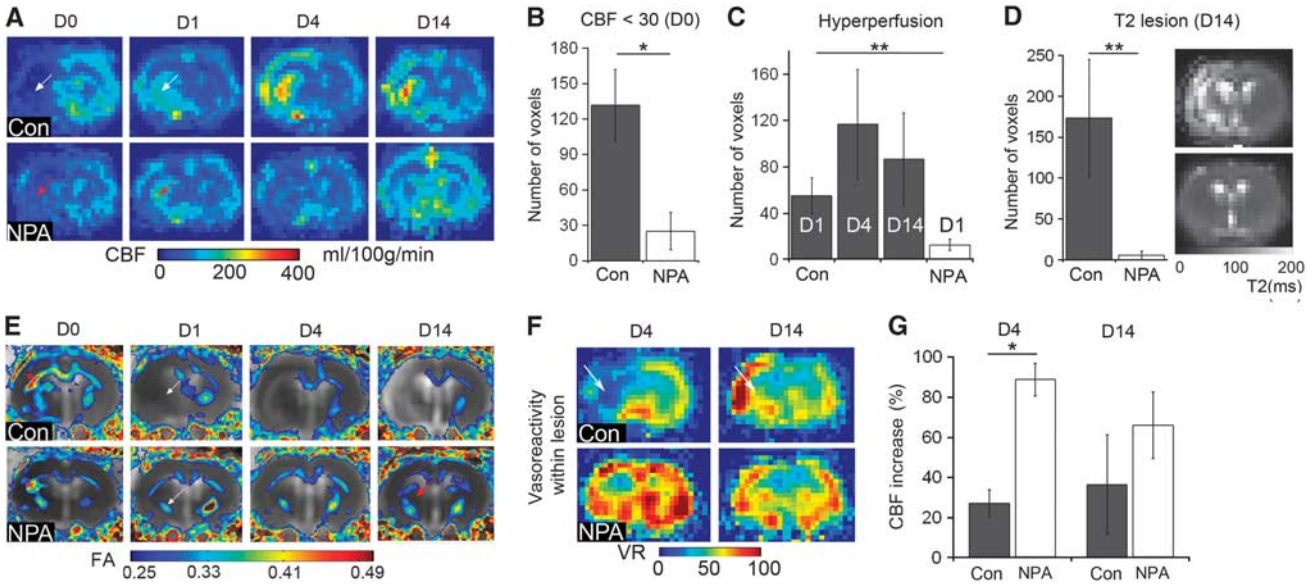

Figure 2. NPA preconditioning results in less severe ischemic perfusion restriction and attenuated tissue damage after stroke. (**A**) Averaged CBF maps from controls (Con) or NPA-treated animals during ischemia (D0) and on days 1, 4, and 14 (D1, D4, D14) demonstrate an attenuated drop in CBF on D0 in the NPA group (red arrow) compared with controls (white arrow). Postischemic hyperperfusion in the NPA group is only observed in few voxels on D1 (red arrow) compared with controls (white arrow). (**B**) CBF < 30: voxels with a CBF value below 30 ml/100 g per minute on D0, resembling severely reduced perfusion. There are significantly less voxels with intraischemic CBF < 30 in the NPA compared with the control group (*$P < 0.05$). (**C**) Number of voxels with postischemic hyperperfusion (CBF > mean + 2 s.d. contralateral) in controls (dark gray columns) and NPA group (white column) at D1, D4, and D14 after reperfusion. There are significantly more hyperperfused voxels in controls than in the NPA- group; the latter with hyperperfusion only on D1 (**$P < 0.011$; D4 and D14 not shown for NPA). (**D**) The number of voxels with an increased T2 value (> mean + 2 s.d. of contralateral), indicating infarct, is significantly higher in controls (**$P < 0.001$) than in NPA animals. To the right, averaged T2 maps from D14 show high signal on the ischemic side in controls, whereas there is barely any signal abnormality detectable in the NPA group. (**E**) Averaged fractional anisotropy (FA) maps from DTI overlaid onto averaged ADC maps on D0, D1, D4, and D14 in the control and NPA group. After a brief episode of increased FA during ischemia (red asterisks), FA is decreased within the area of ischemia (white arrows), indicating derangement of fiber tracts. However, although FA remains low in controls, remaining fiber tracts show a recovery of FA values in NPA animals (red arrow). Also note the development of vasogenic edema, causing an increase in ADC values on the ischemic side in controls, but not in the NPA group. (**F**) Averaged vasoreactivity maps, derived from subtraction of the CBF map acquired during inhalation of air from the CBF map acquired with 5% CO_2 as a vasodilatory stimulus on D4 and D14 in controls and NPA animals. White arrows point to a lack of CBF increase because of 5% CO_2 within the ischemic area in controls on D4, indicating impaired vasoreactivity, which has recovered on D14. Note the overshooting vasoreactivity in peri-lesional, cortical areas in controls on D14, which is present in some but not all animals of the control group. In NPA animals, vasoreactivity within the ischemic area is maintained. (**G**) Vasoreactivity expressed as % increase in CBF with the 5% CO_2 stimulus on D4 and D14 within the voxels with a CBF < 30 mg/100 ml per minute at D0 (severely ischemic voxels). In contrast to NPA-preconditioned animals, vasoreactivity was significantly impaired on D4 in controls (**$P < 0.01$). ADC, apparent diffusion coefficient; CBF, cerebral blood flow; DTI, diffusion tensor imaging; NPA, 3-nitropropionic acid.

ED1 positivity, indicating gliosis and macrophage activation (Figures 4A, 4C, and 4D). Of note, these areas were not detected on T2w MRI, which is the MRI parameter most commonly applied to quantify chronic ischemic damage.[26] This indicates that NPA-induced neuroprotection after stroke is not complete and that regional loss of neurons may occur.

In search for mechanisms of NPA-induced ischemia tolerance, we further analyzed the expression of the K^+/Cl^- co-transporter KCC2 in brains of animals subjected to MCAO with and without NPA preconditioning. KCC2 is upregulated in response to excitotoxic injury, maintaining ion gradients, and supporting neuroprotection[27,28] and downregulated in response to more severe ischemia.[29,30] By preventing excessive intracellular Cl^- accumulation and hyperexcitability after ischemia, KCC2 upregulation might contribute to a protective response elicited by preconditioning. We did not find a specific alteration of the KCC2 expression in preconditioned brains after ischemia; but a decrease in KCC2 signal in the infarct area of both, controls and NPA-preconditioned animals after MCAO (Figure 4A), indicating that postischemic downregulation of KCC2 occurs despite preconditioning in the areas of neuronal damage, most likely reducing GABAergic inhibitory functions.

Structural and Metabolic Adjustments after 3-Nitropropionic Acid Preconditioning

After the robust neuroprotective effect of NPA preconditioning was confirmed in the rat MCAO model, we next sought to characterize changes in the vascular and metabolic properties of animals in the ischemia-tolerant state. In analogy to the MCAO experiments, two groups of animals were either preconditioned with intraperitoneal NPA or saline. Three days later, animals were not subjected to MCAO but analyzed using MRI and histologic analyses of brain tissue. Although NPA preconditioning had no impact on the gross structural integrity, we found a global, approximately 30% reduction in baseline CBF in the NPA group (138.75 ± 19.2 versus 108.6 ± 16.3 mg/100 ml per minute; Figure 5A). Despite this decrease in CBF, VR was preserved (Figure 5B). Another cohort of animals with NPA preconditioning and controls were subjected to HPLC analysis for quantification of metabolites related to mitochondrial function and cell energy state, including adenosine nucleotides (ATP, ADP, and AMP), N-Acetylaspartate, and nicotinamide adenine dinucleotide. In comparison with the saline group, 3 days after NPA preconditioning, tolerant animals had a nonsignificant decrease in ATP (2139.64 ± 220.24 versus 2326.70 ± 180.00 nmol/g wet weight),

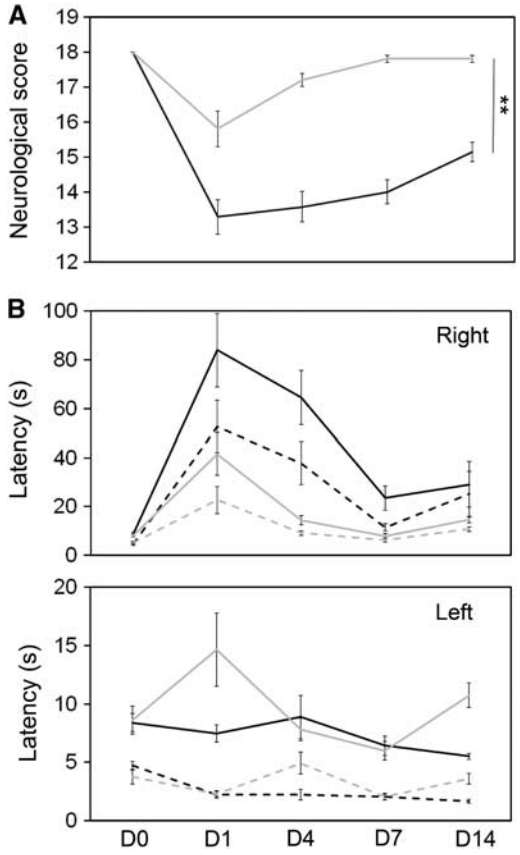

Figure 3. Sensorimotor deficits after MCAO are attenuated by preconditioning. (**A**) In a composite neurologic score where 18 points indicate no deficits and lower scores an impairment of sensorimotor function, NPA (light gray line) animals are significantly less affected than controls (black line) (**$P<0.01$). (**B**) Latency to contact (dashed lines) and remove (solid line) a sticky tape applied to the left or right (indicated in upper right corner of the diagram) forepaw of rats in the control (black) or NPA (light gray) group at different time points before (D0) and after (D1, D4, D7, D14) MCAO. Because of occlusion of the left MCA, the time to contact or remove the tape on the right side is longer in all animals after ischemia. However, on average, deficits are less severe in the NPA group (this effect did not reach significance in repeated measures analysis of variance). MCAO, middle cerebral artery occlusion; NPA, 3-nitropropionic acid.

equal ADP values (259 ± 90.1 versus 207.4 ± 34.5 nmol/g wet weight), a significant increase in AMP (70.51 ± 8.47 versus 47.19 ± 8.28 nmol/g wet weight; $P<0.001$) and an unaltered sum of nucleotides (ATP + ADP + AMP). The change in the concentrations of adenylates caused a significant decrease in the ECP: 0.919 ± 0.016 versus 0.942 ± 0.004; $P<0.01$, indicating a mitochondrial-dependent imbalance in energy production and consumption (Figure 5C). N-Acetylaspartate, a marker of neuronal integrity, was not significantly different between groups (NPA: 8075.2 ± 971.7 versus con 8783.4 ± 513.6), nor was the concentration nicotinamide adenine dinucleotide (NPA: 527.5 ± 68 versus con 550.2 ± 39.7 nmol/g wet weight).

These results suggest that metabolic adjustments might underlie the observed lower CBF in ischemia-tolerant NPA-treated animals. This was supported by a reduced expression of the respiratory chain enzyme cytochrome c-oxidase (COX) in NPA-preconditioned brains (Figures 6A and 6B). To assess possible adaptations at the vascular level, brains of NPA-preconditioned animals and controls underwent immunofluorescence analysis of the endothelial marker RECA-1 3 days after treatment. We did not find a significant difference in RECA-1 expression between groups in any of the regions analyzed (cortex, striatum, dentate gyrus; Figures 6A and 6B). We again analyzed brain KCC2 expression 3 days after NPA preconditioning without MCAO. We found no significant difference in KCC2 expression between NPA animals or controls in any of the three regions analyzed (Figures 6A and 6B). This argues against a role of KCC2 as part of the NPA-preconditioning signal. No signs of neuronal damage were detected in both groups with NeuN, MAP2- or caspase-3 stain for apoptotic cells (data not shown).

DISCUSSION

The mechanisms by which a preconditioned brain maintains tolerance to ischemia remain obscure, especially the contribution of vascular versus metabolic adaptations. We approached this problem by analyzing CBF and metabolic phosphates in NPA-preconditioned rats at the time of ischemia tolerance. Furthermore, infarct growth and functional outcomes were assessed after MCAO in preconditioned and sham-preconditioned rats.

MRI during and after MCAO in the NPA-mediated model of pharmacological preconditioning revealed that NPA-mediated protection of the brain started immediately during the ischemic challenge through maintenance of intraischemic blood flow and recovery of the initial MCAO-induced cytotoxic edema. As a consequence, structural tissue integrity was preserved, which was reflected by only slight and temporary disruption of fiber tracts in diffusion tensor imaging, normal VR, and less vasogenic edema with significantly smaller final T2-lesions. When CBF was measured in the ischemia-tolerant animals (72 hours after NPA preconditioning), we found a significant global reduction in CBF with preserved VR. Strikingly similar to our results, in a rat model of ischemia tolerance induced by cortical spreading depression, autoradiography demonstrated a CBF reduction restricted to those regions affected by cortical spreading depression to a similar extent and at a similar time (72 hours after cortical spreading depression) before ischemia.[31] Laser Doppler flowmetry was suggestive of preserved intraischemic CBF in tolerant animals; however, the limitations of this technique including a lower spatial resolution and relative CBF measurements led the authors to hypothesize that based on the lower preischemic CBF, absolute values might not have been higher in CSD-preconditioned animals. These findings support a common mechanism of ischemia tolerance where metabolic adaptations are first installed which later facilitate preserved vascular responses to ischemia. Only few studies have investigated changes in CBF because of preconditioning before and at the time of subsequent ischemia. After preconditioning, some groups have found an increase in relative CBF, as determined from laser Doppler flowmetry, during or in the hours after subsequent ischemia,[32–34] whereas others observed neuroprotection without CBF effects during MCAO.[35–37] Dawson *et al* used autoradiography to show that 15 minutes after the onset of MCAO, CBF was unchanged in animals subjected to lipopolysaccharide preconditioning; however, 4 and 24 hours later, microvascular perfusion as assessed by an intravascular fluorescent tracer technique was preserved at higher levels in preconditioned animals compared with controls.[38] Gustavsson *et al* observed an attenuation of the CBF decrease during a hypoxic/ischemic injury 24 hours after hypoxic preconditioning, along with an increase in microvascular density,[9] albeit in a neonatal model where angiogenesis is likely to remain more plastic compared with the adult brain. In our model, no increase in vascularization was observed in ischemia-tolerant brains, however, the lower ECP and reduced COX expression pattern suggested a significant decrease in mitochondrial phosphorylation capacity at the rate necessary to meet the cellular energy demand subsequent to NPA administration.

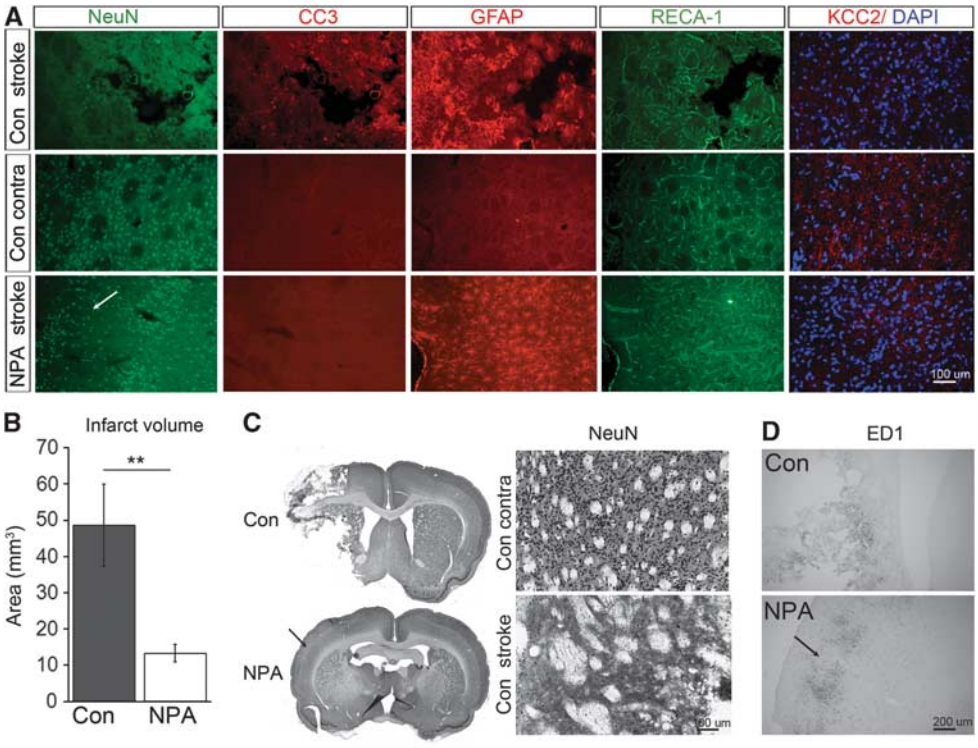

Figure 4. Ischemic lesions after MCAO in controls (Con) and NPA-preconditioned animals. (**A**) Representative immunofluorescence images demonstrating expression of NeuN (green), CC3 (red), GFAP (red), RECA-1 (green), and KCC2 overlaid onto DAPI (red and blue) on the ipsilateral (stroke) and contralateral (contra) side in controls (upper and middle panel) as well as on the ipsilateral (stroke) side in NPA-preconditioned animals (lower panel). Two weeks after MCAO, tissue necrosis has occurred in controls, whereas only selective neuronal damage can be detected in NPA animals (white arrow on the lower panel NeuN staining). (**B**) Infarct size derived from NeuN immunohistochemistry in Con and NPA animals. Note that this analysis includes areas of cystic tissue degeneration as well as selective neuronal loss. (**C**) Left: overview ($\times$ 2) of NeuN immunohistochemistry in a Con (upper panel) versus NPA (lower panel) animal. Right: higher ($\times$ 10) magnification of the NeuN immunohistochemistry in a control animal showing normal striatal NeuN expression on the contralateral (upper panel) and loss of NeuN expression on the ipsilateral (lower panel) side. (**D**) ED1 immunohistochemistry demonstrating macrophage infiltration at the infarct border in controls (upper panel) and at the zones of selective neuronal death in NPA animals (lower panel). Arrows in **C** and **D** indicate areas of selective neuronal damage in NPA animals. DAPI, 4,6-diamidino-2-phenylindole 4,6-diamidino-2-phenylindole; MCAO, middle cerebral artery occlusion; NPA, 3-nitropropionic acid.

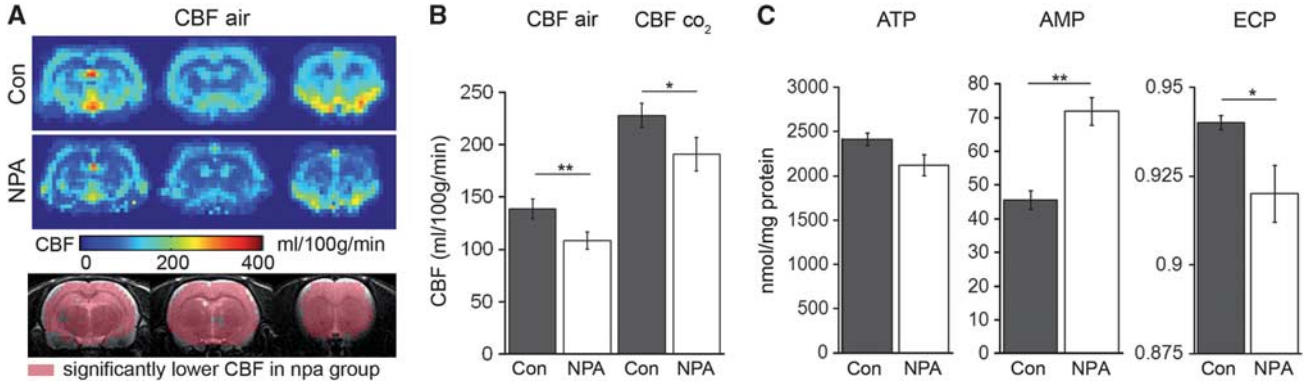

Figure 5. The ischemia-tolerant state is characterized by lower baseline CBF and energy imbalance in NPA-preconditioned animals. (**A**) Average CBF maps from controls (Con) and NPA-preconditioned (NPA) animals 3 days after saline or NPA treatment without the induction of experimental stroke. Lower panel: voxel-wise statistics of CBF values between groups indicating voxels with significantly lower CBF in NPA animals in pink, overlaid onto anatomic (T2w) images. There is a global CBF reduction 3 days after NPA treatment compared with controls. (**B**) Comparison of whole-brain CBF values between groups with and without CO_2 challenge. Although baseline CBF is lower in NPA animals, CBF increases to a similar extent after application of CO_2, which indicates that vasoreactivity is preserved after NPA treatment. (**C**) Levels of the brain metabolites ATP, AMP, and ECP 3 days after NPA preconditioning or sham treatment. There is significantly more AMP and a lower ECP in brains of the NPA group. AMP, adenosine monophosphate; ATP, adenosine triphosphate; CBF, cerebral blood flow; ECP, energy charge potential; NPA, 3-nitropropionic acid.

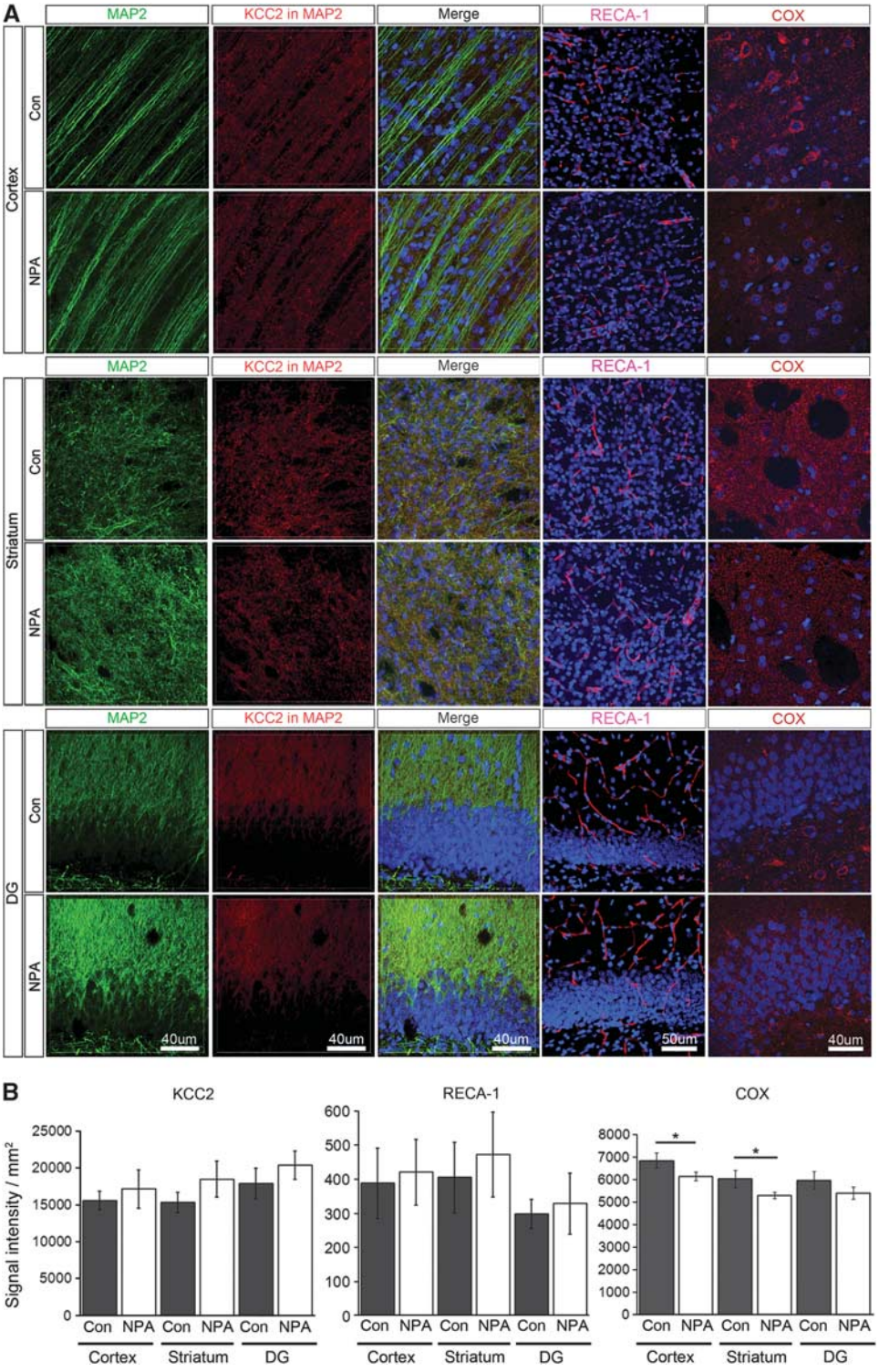

Figure 6. NPA preconditioning decreases the expression of COX, but does not influence the density of blood vessels or the expression of the chloride co-transporter KCC2. (**A**) Panels are showing MAP2 (green), KCC2 (red), RECA-1 (red), and COX (red) expression in the cortex (upper panels), striatum (middle panels), and dentate gyrus (DG, lower panels) of an exemplary control and NPA animal. Nuclei were counterstained with DAPI (blue). MAP2: MAP2 expression (green), KCC2 in MAP2: KCC2 signal (red) extracted from the MAP2-masked area, Merge: overlays of MAP2, KCC2, and DAPI. RECA-1: overlay of RECA-1 expression (red) and DAPI (blue). COX: overlay of COX expression (red) and DAPI (blue). (**B**) Quantitative analyses of the KCC2 (left), RECA-1 (center), and COX (right) immunofluorescence signal in cortex, striatum, and DG in controls and NPA (mean ± s.d.). DAPI, 4,6-diamidino-2-phenylindole 4,6-diamidino-2-phenylindole; NPA, 3-nitropropionic acid.

In addition, the decrease in the rate of ATP synthesis provoked a change in the proportion of adenosine nucleotides suggesting a state of energy imbalance that has been shown to be associated with induction of cellular programs for neuroprotection.[39] Our finding of decreased ECP together with the reduction of CBF throughout the brain of NPA-preconditioned animals is a strong

argument supporting a role of energy metabolism imbalance for preconditioning, as suggested by the tendency to decrease the rate of ATP synthesis with a concomitant increase in its dephosphorylated products (AMP). As metabolites in our experiments were measured in whole-brain homogenates, it is possible that apparently the modest differences found in these parameters might have been of larger amplitude in a small metabolically active compartment such as neuron terminals.

Albeit to a much lesser extent, such response might be similar to the prolonged energy conserving phase of topor in hibernating animals.[40] The analogy between ischemia tolerance in hibernators and tolerance induced by preconditioning has long been suggested by similar neuroprotective mechanisms, such as the induction of HIF-dependent pathways, adenosine receptor activation, and the reduction of glutamate release.[1,41] However, the role of metabolic downregulation in preconditioning-induced tolerance has remained open.[5,42–44] On the basis of our results, it is not possible to discriminate if the observed metabolic adjustments occurred directly because of the inhibition of succinate dehydrogenase by NPA, or later. Interestingly, although the inhibition of succinate dehydrogenase after NPA application is immediate (30 minutes) and longer lasting (3 days), the direct effect of NPA on ATP synthesis is much shorter lasting (approximately 2 hours).[11]

Histologic analysis proved the NPA-induced tissue protection suggested from MRI, however, selective neuronal death occurred in parts of the ischemic territory that were not detected on T2w MRI. This finding points out the importance of multimodal (imaging/functional testing/histology) readouts in the assessment of ischemic damage. Although our findings may be specific for preconditioning with NPA, evidence from other preconditioning paradigms speak for common principal mechanisms, such as induction of Bcl-2, ATP-dependent potassium channels and TNFα.[7,45,46] Future experiments will be needed to test additional models of preconditioning using longitudinal, quantitative CBF measurements.

Current outcome prediction algorithms for stroke are based on preexisting, non-modifiable patient characteristics.[47] On the basis of the findings presented here, MRI-based approaches will be able to refine these parameters and have the potential to guide future therapeutic decisions by analyzing preischemic or intraischemic CBF, postischemic hyperperfusion, and early diffusion-weighted imaging lesion dynamics.

DISCLOSURE/CONFLICT OF INTEREST

The authors declare no conflict of interest.

REFERENCES

1 Kitagawa K. Ischemic tolerance in the brain: endogenous adaptive machinery against ischemic stress. *J Neurosci Res* 2012; **90**: 1043–1054.
2 Schaller B. Ischemic preconditioning as induction of ischemic tolerance after transient ischemic attacks in human brain: its clinical relevance. *Neurosci Lett* 2005; **377**: 206–211.
3 Wegener S, Gottschalk B, Jovanovic V, Knab R, Fiebach JB, Schellinger PD *et al.* Transient ischemic attacks before ischemic stroke: preconditioning the human brain? A multicenter magnetic resonance imaging study. *Stroke* 2004; **35**: 616–621.
4 Rezkalla SH, Kloner RA. Preconditioning in humans. *Heart Fail Rev* 2007; **12**: 201–206.
5 Dirnagl U, Becker K, Meisel A. Preconditioning and tolerance against cerebral ischaemia: from experimental strategies to clinical use. *Lancet Neurol* 2009; **8**: 398–412.
6 Stevens SL, Leung PY, Vartanian KB, Gopalan B, Yang T, Simon RP *et al.* Multiple preconditioning paradigms converge on interferon regulatory factor-dependent signaling to promote tolerance to ischemic brain injury. *J Neurosci* 2011; **31**: 8456–8463.
7 Gidday JM. Cerebral preconditioning and ischaemic tolerance. *Nat Rev Neurosci* 2006; **7**: 437–448.
8 Kirino T. Ischemic tolerance. *J Cereb Blood Flow Metab* 2002; **22**: 1283–1296.
9 Gustavsson M, Mallard C, Vannucci SJ, Wilson MA, Johnston MV, Hagberg H. Vascular response to hypoxic preconditioning in the immature brain. *J Cereb Blood Flow Metab* 2007; **27**: 928–938.
10 Gidday JM. Pharmacologic Preconditioning: translating the Promise. *Transl Stroke Res* 2010; **1**: 19–30.
11 Wiegand F, Liao W, Busch C, Castell S, Knapp F, Lindauer U *et al.* Respiratory chain inhibition induces tolerance to focal cerebral ischemia. *J Cereb Blood Flow Metab* 1999; **19**: 1229–1237.
12 Weih M, Bergk A, Isaev NK, Ruscher K, Megow D, Riepe M *et al.* Induction of ischemic tolerance in rat cortical neurons by 3-nitropropionic acid: chemical preconditioning. *Neurosci Lett* 1999; **272**: 207–210.
13 Horiguchi T, Kis B, Rajapakse N, Shimizu K, Busija DW. Opening of mitochondrial ATP-sensitive potassium channels is a trigger of 3-nitropropionic acid-induced tolerance to transient focal cerebral ischemia in rats. *Stroke* 2003; **34**: 1015–1020.
14 Zhu HC, Gao XQ, Xing Y, Sun SG, Li HG, Wang YF. Inhibition of caspase-3 activation and apoptosis is involved in 3-nitropropionic acid-induced ischemic tolerance to transient focal cerebral ischemia in rats. *J Mol Neurosci* 2004; **24**: 299–305.
15 Koizumi J, Yoshida Y, Nakazawa T, Ohneda G. Experimental studies of ischemic brain edema, I: a new experimental model of cerebral embolism in rats in which recirculation can be introduced in the ischemic area. *Jpn J Stroke* 1986; **8**: 1–8.
16 Wegener S, Wong EC. Longitudinal MRI studies in the isoflurane-anesthetized rat: long-term effects of a short hypoxic episode on regulation of cerebral blood flow as assessed by pulsed arterial spin labelling. *NMR Biomed* 2008; **21**: 696–703.
17 Wegener S, Artmann J, Luft AR, Buxton RB, Weller M, Wong EC. The time of maximum post-ischemic hyperperfusion indicates infarct growth following transient experimental ischemia. *PLoS One* 2013; **8**: e65322.
18 Wong EC, Buxton RB, Frank LR. Quantitative imaging of perfusion using a single subtraction (QUIPSS and QUIPSS II). *Magn Reson Med* 1998; **39**: 702–708.
19 Wegener S, Wu WC, Perthen JE, Wong EC. Quantification of rodent cerebral blood flow (CBF) in normal and high flow states using pulsed arterial spin labeling magnetic resonance imaging. *J Magn Reson Imaging* 2007; **26**: 855–862.
20 Modo M, Rezaie P, Heuschling P, Patel S, Male DK, Hodges H. Transplantation of neural stem cells in a rat model of stroke: assessment of short-term graft survival and acute host immunological response. *Brain Res* 2002; **958**: 70–82.
21 Wegener S, Weber R, Ramos-Cabrer P, Uhlenkueken U, Wiedermann D, Kandal K *et al.* Subcortical lesions after transient thread occlusion in the rat: T2-weighted magnetic resonance imaging findings without corresponding sensorimotor deficits. *J Magn Reson Imaging* 2005; **21**: 340–346.
22 Garcia JH, Wagner S, Liu KF, Hu XJ. Neurological deficit and extent of neuronal necrosis attributable to middle cerebral artery occlusion in rats. Statistical validation. *Stroke* 1995; **26**: 627–634, discussion 635.
23 Lazzarino G, Nuutinen M, Tavazzi B, Di Pierro D, Giardina B. A method for preparing freeze-clamped tissue samples for metabolite analyses. *Anal Biochem* 1989; **181**: 239–241.
24 Lazzarino G, Amorini AM, Fazzina G, Vagnozzi R, Signoretti S, Donzelli S *et al.* Single-sample preparation for simultaneous cellular redox and energy state determination. *Anal Biochem* 2003; **322**: 51–59.
25 Tavazzi B, Lazzarino G, Leone P, Amorini AM, Bellia F, Janson CG *et al.* Simultaneous high performance liquid chromatographic separation of purines, pyrimidines, N-acetylated amino acids, and dicarboxylic acids for the chemical diagnosis of inborn errors of metabolism. *Clin Biochem* 2005; **38**: 997–1008.
26 van Dorsten FA, Olah L, Schwindt W, Grune M, Uhlenkuken U, Pillekamp F *et al.* Dynamic changes of ADC, perfusion, and NMR relaxation parameters in transient focal ischemia of rat brain. *Magn Reson Med* 2002; **47**: 97–104.
27 Pellegrino C, Gubkina O, Schaefer M, Becq H, Ludwig A, Mukhtarov M *et al.* Knocking down of the KCC2 in rat hippocampal neurons increases intracellular chloride concentration and compromises neuronal survival. *J Physiol* 2011; **589**(Pt 10): 2475–2496.
28 Blaesse P, Airaksinen MS, Rivera C, Kaila K. Cation-chloride cotransporters and neuronal function. *Neuron* 2009; **61**: 820–838.
29 Jaenisch N, Witte OW, Frahm C. Downregulation of potassium chloride cotransporter KCC2 after transient focal cerebral ischemia. *Stroke* 2010; **41**: e151–e159.
30 Galeffi F, Sah R, Pond BB, George A, Schwartz-Bloom RD. Changes in intracellular chloride after oxygen-glucose deprivation of the adult hippocampal slice: effect of diazepam. *J Neurosci* 2004; **24**: 4478–4488.
31 Otori T, Greenberg JH, Welsh FA. Cortical spreading depression causes a long-lasting decrease in cerebral blood flow and induces tolerance to permanent focal ischemia in rat brain. *J Cereb Blood Flow Metab* 2003; **23**: 43–50.
32 Kunz A, Park L, Abe T, Gallo EF, Anrather J, Zhou P *et al.* Neurovascular protection by ischemic tolerance: role of nitric oxide and reactive oxygen species. *J Neurosci* 2007; **27**: 7083–7093.
33 Fan YY, Hu WW, Dai HB, Zhang JX, Zhang LY, He P *et al.* Activation of the central histaminergic system is involved in hypoxia-induced stroke tolerance in adult mice. *J Cereb Blood Flow Metab* 2011; **31**: 305–314.

34 Furuya K, Zhu L, Kawahara N, Abe O, Kirino T. Differences in infarct evolution between lipopolysaccharide-induced tolerant and nontolerant conditions to focal cerebral ischemia. *J Neurosurg* 2005; **103**: 715–723.
35 Barone FC, White RF, Spera PA, Ellison J, Currie RW, Wang X *et al.* Ischemic preconditioning and brain tolerance: temporal histological and functional outcomes, protein synthesis requirement, and interleukin-1 receptor antagonist and early gene expression. *Stroke* 1998; **29**: 1937–1950, discussion 1950–1951.
36 Alkayed NJ, Goyagi T, Joh HD, Klaus J, Harder DR, Traystman RJ *et al.* Neuroprotection and P450 2C11 upregulation after experimental transient ischemic attack. *Stroke* 2002; **33**: 1677–1684.
37 Matsushima K, Hakim AM. Transient forebrain ischemia protects against subsequent focal cerebral ischemia without changing cerebral perfusion. *Stroke* 1995; **26**: 1047–1052.
38 Dawson DA, Furuya K, Gotoh J, Nakao Y, Hallenbeck JM. Cerebrovascular hemodynamics and ischemic tolerance: lipopolysaccharide-induced resistance to focal cerebral ischemia is not due to changes in severity of the initial ischemic insult, but is associated with preservation of microvascular perfusion. *J Cereb Blood Flow Metab* 1999; **19**: 616–623.
39 Di Pietro V, Amorini AM, Tavazzi B, Hovda DA, Signoretti S, Giza CC *et al.* Potentially neuroprotective gene modulation in an in vitro model of mild traumatic brain injury. *Mol Cell Biochem* 2013; **375**: 185–198.
40 Dave KR, Christian SL, Perez-Pinzon MA, Drew KL. Neuroprotection: lessons from hibernators. *Comp Biochem Physiol B Biochem Mol Biol* 2012; **162**: 1–9.
41 Narayanan SV, Dave KR, Perez-Pinzon MA. Ischemic preconditioning and clinical scenarios. *Curr Opin Neurol* 2013; **26**: 1–7.
42 Yenari M, Kitagawa K, Lyden P, Perez-Pinzon M. Metabolic downregulation: a key to successful neuroprotection? *Stroke* 2008; **39**: 2910–2917.
43 Kapinya KJ, Lowl D, Futterer C, Maurer M, Waschke KF, Isaev NK *et al.* Tolerance against ischemic neuronal injury can be induced by volatile anesthetics and is inducible NO synthase dependent. *Stroke* 2002; **33**: 1889–1898.
44 Dornbos 3rd D, Zwagerman N, Guo M, Ding JY, Peng C, Esmail F *et al.* Preischemic exercise reduces brain damage by ameliorating metabolic disorder in ischemia/reperfusion injury. *J Neurosci Res* 2013; **91**: 818–827.
45 Kato K, Shimazaki K, Kamiya T, Amemiya S, Inaba T, Oguro K *et al.* Differential effects of sublethal ischemia and chemical preconditioning with 3-nitropropionic acid on protein expression in gerbil hippocampus. *Life Sci* 2005; **77**: 2867–2878.
46 Nakagawa I, Ogawa Y, Noriyama Y, Nakase H, Yamashita M, Sakaki T. Chemical preconditioning prevents paradoxical increase in glutamate release during ischemia by activating ATP-dependent potassium channels in gerbil hippocampus. *Exp Neurol* 2003; **183**: 180–187.
47 Flint AC, Faigeles BS, Cullen SP, Kamel H, Rao VA, Gupta R *et al.* THRIVE score predicts ischemic stroke outcomes and thrombolytic hemorrhage risk in VISTA. *Stroke* 2013; **44**: 3365–3369.